Plasmonics (2022) 17:823–829
https://doi.org/10.1007/s11468-021-01590-8

A Terahertz Tunable Metamaterial Reflective Polarization Converter Based On Vanadium Oxide Film

Fu-yuan Yu[1] · Xiong-jun Shang[2] · Wei Fang[1] · Qing-qing Zhang[1] · Yan Wu[1] · Wang Zhao[1] · Jia-fang Liu[1] · Qing-qing Song[1] · Cheng Wang[1] · Jia-bing Zhu[1] · Xiao-bo Shen[1]

Received: 21 June 2021 / Accepted: 17 December 2021 / Published online: 8 January 2022

Abstract
In this paper, on the basis of metamaterial, a simply single-layer and tunable reflective polarization converter has been numerically investigated, which is composed of vanadium dioxide film (VO_2) component combined with two-corner-cut square patch cut by a slit and reflective ground layer. Calculated results obtained by the CST Microwave Studio show that in the frequency of 2.22–5.42 THz, high polarization conversion efficiency (polarization conversion ratio (*PCR*) above 90%) can be normally achieved at the temperature about 25 °C for both the linearly and circularly polarized wave incidence. At the same time, the cross-polarization converter can be analyzed and obtained from the view on qualitative variable of polarization azimuth angle (θ) and ellipticity (η). Moreover, a tunable polarization conversion property can be realized by the designed device with vanadium dioxide utilizing changing different conductivities. Even so, to be demonstrated, the physical mechanism of the merits of controllability and uniqueness has been discussed by the distributions of current densities and E-field map, respectively. According to the prior results, the designed metamaterial could be applied in the area of temperature-controlled sensing, THz wireless communication, tunable polarized devices.

Keywords Polarization converter · Vanadium dioxide · Metamaterial

Introduction

Polarization has become such an enormous important property of the electric–magnetic wave that it can provide real application in information processing, imaging, and sensing [1–4]. As a fundamental device, polarization converter, that is traditionally accomplished by natural birefringent material or dichroic crystals, has become acquiring more and more attentions from researchers in different areas. The results could be attributed to the advent of metamaterials (MMs), of which the ability is not only overcome shortcomings of the effect weakly and the volume bulky incurred by traditional materials but also open a promising platform to control the polarization states of light [5, 6]. With regard to MM converter, many interesting phenomena have been reported in THz spectrum, such as dual-band [7], tri-band [8], multi-band [9], and broadband [10, 11] polarization converter. However, only a few attempts have been implemented to realize dynamic modulation.

Actually, to our knowledge, phase change materials (PCMs) including GeSbTe (GST) [12], graphene [13], semiconductors [14], and vanadium dioxide (VO_2) [15–18] are capable of accomplishing the phase modulation excited by external factors, for instance electric bias, temperature, and photo excitation. Thus, the MMs integrated with dynamic such inclusions above mentioned can accomplish tunable polarization conversion modulation. Currently, among PCMs, since the studied structure was developed and improved using VO_2 [19, 20], there must be more stress on the properties, critical temperature, and other important factors of that. It is well-known that VO_2 exhibits an insulator-to-metal phase transition [21, 22] due to changeable conductivity depending on the various temperatures. Based on this point, a tunable polarization

✉ Fu-yuan Yu
fuyhfut@126.com

1 School of Electronic Engineering, Huainan Normal University, Huainan 232038, People's Republic of China

2 Hunan Provincial Key Laboratory of Flexible Electronic Materials Genome Engineering, School of Physics and Electronic Science, Changsha University of Science and Technology, Changsha 410004, People's Republic of China

converter with superior performance becomes more and more anticipated. In [15, 18, 19], authors provide analogical multi-layer metamaterial device, among which the middle VO_2 layer behaves as absorptance or reflectance at the metal phase. In [16], the polarization converter works merely at the specific frequency of 0.468 and 0.502 THz with the phase transition of VO_2, respectively. However, previous works rarely focus on simple and single-layer polarization converter device characterized with high polarization conversion efficiency within relatively broad absolute bandwidth in THz regime to our knowledge. In contrast, our manuscript has proposed and demonstrated this point.

Stimulated by essential need above, a simply single-layer and tunable reflective polarization converter based on metamaterial is proposed in THz spectrum, which consists of vanadium dioxide film (VO_2) inserted by a two-corner-cut square patch resonator with a slit and reflective ground layer. Numerical calculation shows that high polarization conversion properties can be quantitatively described by polarization conversion ratio (*PCR*) and qualitatively confirmed by polarization azimuth angle (θ) and ellipticity (η). According to analyzed results, cross-polarized conversion occurs at three resonant peaks (2.39, 3.78, and 5.27 THz) along with high *PCR* (above 90%) in the frequency of 2.22 to 5.42 THz. Thereafter, to obtain tunable polarization conversion performance, the frequency spectrum characteristics of *PCR* can be gradually varied from high tri-band to eventually unity close to nearly zero with increases of conductivities of VO_2 and verified by distributions of current densities. Last but not least, the reason for specific superior performance due to a slit has been illustrated in comprehensively. Therefore, such dynamic changes of phase transition metamaterial offer a new route for acquiring multifunctional devices, such as switches and polarization modulators.

Descriptions of the Designed MMs and Simulation Model

The proposed MMs (Fig. 1(a)) consist of periodical identical unit cells (Fig. 1(b)) which composed of hybrid layer and metallic ground layer separated by polyimide dielectric layer with a relative dielectric constant of 3.5 [23] and a thickness (t1) of 10 μm (Fig. 1(d)), as schematically shown in Fig. 1(c). Obviously, the hybrid layer (first layer) comprises a metallic two-corner-cut square patch resonator with a slit and VO_2 film. The top and bottom

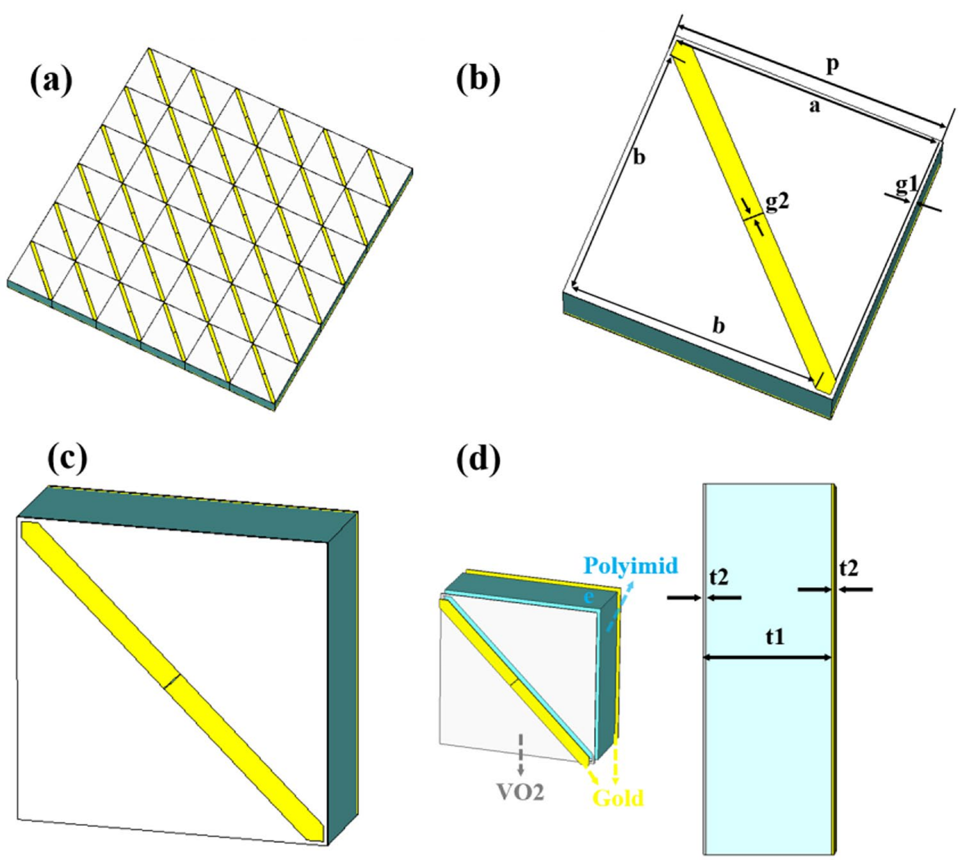

Fig. 1 Schematic diagram of the designed polarization converter. (**a**) Titled extended periodic array view, (**b**) magnified front view of a unit cell, (**c**) perspective view of a unit cell, (**d**) right view of a unit cell

metallic layers are made by the same gold dealt with the Drude model ($\omega_p = 2\pi \times 2175$ THz, $\omega_c = 2\pi \times 4.35$ THz) [24] and the thickness (t2) of 0.2 μm. Among the hybrid layer, the properties of VO_2 film can be expressed by the Bruggeman effective model [25, 26]:

$$\varepsilon(VO2) = \frac{1}{4}\left\{\varepsilon_d(2-3V) + \varepsilon_m(3V-1) + \sqrt{\left[\varepsilon_d(2-3V) + \varepsilon_m(3V-1)^2 + 8\varepsilon_d\varepsilon_m\right]}\right\}, \quad (1)$$

where ε_d and ε_m denote dielectric constants of the insulating and metallic phase, respectively. Moreover, V indicates the volume fraction of the metallic regions. According to the above parameters, generally, the complex dielectric constant of VO_2 in THz frequency domain can be described by the Bruggeman effective-medium theory (EMT). Also, for simplicity, the conductivity of VO_2 can alternatively characterize dynamic insulator-to-metal phase change of VO_2 films [17, 27, 28]. Thus, in our simulation, the relative permittivity and conductivity of VO_2 can be set as 9 [25] and 200 S/m [25] at the temperature about 25 °C, respectively. All the designs, of which the relevant other parameter given below (Table 1), can be carried out by CST Microwave Studio based on frequency domain solver. Periodic boundary condition and port boundary condition are applied to X/Y direction and Z direction, respectively.

To better understand the performance of the designed polarization converter, the polarization conversion ratio (*PCR*) can be adopted. Concerning the polarization of incident wave that exists along the *y*-direction, the *PCR* can be calculated by Eq. (2) as follows. Moreover, for the *x*-polarized wave incidence, the subscripts about *x* and *y* in Eq. (2) can be merely interchanged:

$$PCR = \frac{\left|r_{xy}\right|^2}{\left|r_{xy}\right|^2 + \left|r_{yy}\right|^2}, \quad (2)$$

where $r_{xy} = E_{rx}/E_{iy}$ and $r_{yy} = E_{ry}/E_{iy}$ are reflective coefficients for cross-polarized and co-polarized wave. The alphabet *i* and *r* denote incidence and reflection, respectively. For the incident circular polarization, the subscripts about *y* and *x* can be replaced *L* and *R*, respectively.

Results and Discussions

Discussion of Fixed Metasurface Device

To characterize polarization conversion performance of the designed MMs, the reflective amplitude ($|r_{ij}|$) and PCR_i for linear and circular polarization incident wave have been investigated, respectively. The subscript *i* and *j* represent either *x*, *y* or *R*, *L*. As exhibited in Fig. 2(a), cross-reflective coefficients $|r_{xy}|$ and $|r_{yx}|$ indicate the same characteristics which hold above 0.85 from around 2.22 and 5.42 THz. At the same time, it is worth noticing that the curves of cross-reflection coefficients exist three resonant peaks at 2.39, 3.78, and 5.27 THz, while both the co-polarized reflective coefficients $|r_{xx}|$ and $|r_{yy}|$ are much lower than cross-polarized $|r_{yx}|$ and $|r_{xy}|$, where especially beneath 0.07 at frequency of 2.39, 3.78, and 5.27 THz. In other words, nearly total the *y*- (*x*-) polarized wave could be converted the cross polarized, i.e., *x*- (*y*-) polarized wave at the three resonant peaks. The conclusion can also be furtherly inferred from Fig. 2(b) that the *PCR* more than 0.99 stands at the nearby frequency points of 2.39, 3.78, and 5.27 THz due to the resonant effects, while high polarization conversion efficiency (*PCR* above 0.9) can be quantitatively achieved with broad frequency domain from 2.22 to 5.42 THz. In addition, more interesting phenomenon can be witnessed from Fig. 2(c) and (d) that the reflective parameters under circular polarized wave keep same trends with the reflective parameters under linear polarized wave, namely, $|r_{xy}| = |r_{yx}| = |r_{RL}| = |r_{LR}|$, $|r_{xx}| = |r_{yy}| = |r_{RR}| = |r_{LL}|$, and $PCR(y) = PCR(x) = PCR(R) = PCR(L)$. Based on analysis above, the designed MMs can be acted as linear polarization as well as circular polarization converter.

To better qualitatively verdict the polarization state of electromagnetic wave under normal illumination, the formula can be expressed as follows [24]:

$$\theta = \frac{1}{2}\arctan\left(\frac{2p_r\cos(\varphi_r)}{1 - |p_r|^2}\right), \quad (3)$$

$$\eta = \frac{1}{2}\arcsin\left(\frac{2p_r\sin(\varphi_r)}{1 + |p_r|^2}\right), \quad (4)$$

where $p_r = |r_{xy}|/|r_{yy}|$ and $\varphi_r = \arg(r_{xy}) - \arg(r_{yy})$. The θ denotes the angle between reflective and incident polarization plane, while the η characterizes the polarization state of the reflective wave. When the $\eta = 0°$ and $\theta \neq 90°$, the reflective wave

Table 1 All dimension parameters of the designed polarization converter

Parameters	P	a	b	g1	g2	t1	t2
Value (μm)	30	29.2	27.6	0.4	0.2	10	0.2

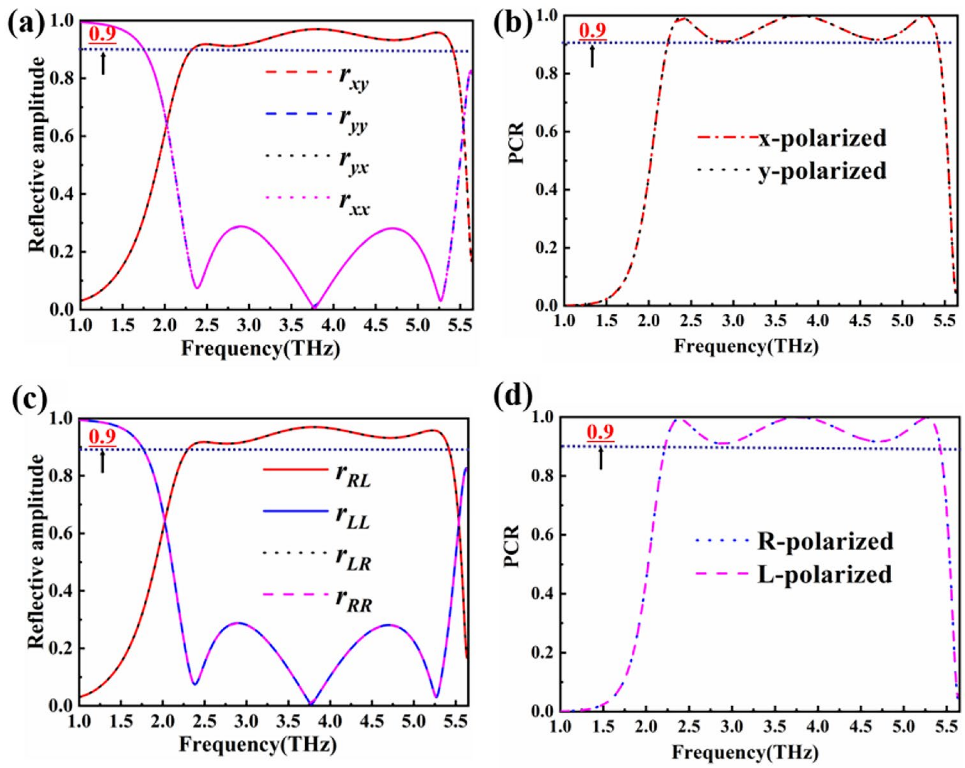

Fig. 2 (**a**) Simulated reflective coefficient and (**b**) *PCR* for incident linear polarization. (**c**) Simulated reflective coefficient and (**d**) *PCR* for incident circular polarization

keep linear polarization state with an angle of θ referred to the incident wave, but not cross-polarization state. What is more, the pure cross-polarization wave can be obtained when $\eta = 0°$ and $\theta = 90°$. As is shown in Fig. 3, the ellipticity η of the incident *y*-polarized wave stands less than 18° from 2.22 to 5.42 THz at whole frequency band and keeps nearly 0° at the around resonant frequency of 2.39, 3.78, and 5.27 THz. The deep meaning implies that a near linear polarization wave is obtained around the three resonant frequencies. Moreover, furtherly the cross-polarization conversion can be maintained when the polarization azimuth angle θ keeps $\pm 90°$ at the same three resonate frequency points in Fig. 3.

Discussion of Changeable Metasurface Device

To further obtain interesting dynamic tunable reflective polarization conversion for the enhanced hybrid metamaterial, more

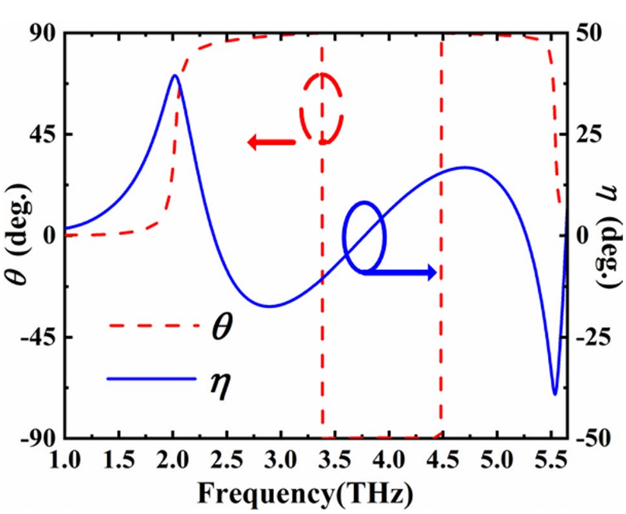

Fig. 3 The polarization azimuth angle (θ) and ellipticity (η) under the normal incident *y*-polarized wave

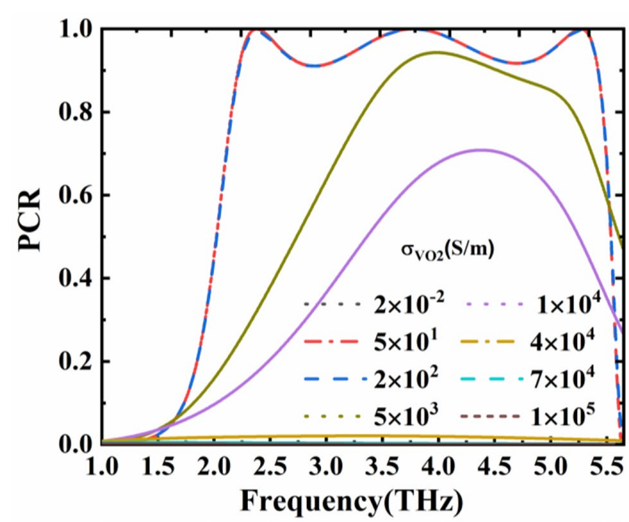

Fig. 4 The *PCR* of incident *y*-polarized wave under the different VO_2 film conductivities

attentions have been paid on the specific kind thermal material, i.e., VO_2. As we all know, the conductivities for VO_2 film change with the changeable temperature, thus resulting into incident electromagnetic wave phase-transition when VO_2 film acts as from insulator state to metallic state. To be concreted, the VO_2 film exhibits an insulating state when the value for conductivity is lower than 200 S/m controlled by the temperature labeled with 25 °C, while shows an metallic state with the conductivity exceed higher than 10^5 S/m attained at the temperature of 85 °C [25]. To be convinced, as is demonstrated in Fig. 4, the *PCR* for incident *y*-polarized wave decreases obviously with the conductivity increasing from 200 to 10^5 S/m. Eventually, the *PCR* is almost 0 when the VO_2 film is metal state with the conductivity set as 10^5 S/m. That means almost all of the incident *y*-polarized components penetrate through the top hybrid layer and could be transformed into *x*-polarized component when $\sigma_{VO2} = 200$ S/m at the temperature of 25 °C. However, the incident *y*-polarized component reflects by the top hybrid layer when $\sigma_{VO2} = 10^5$ S/m at the temperature of 85 °C. According to such analysis above, it can be concluded that actively dynamic changeable polarization conversion device can be designed based on MMs with VO_2.

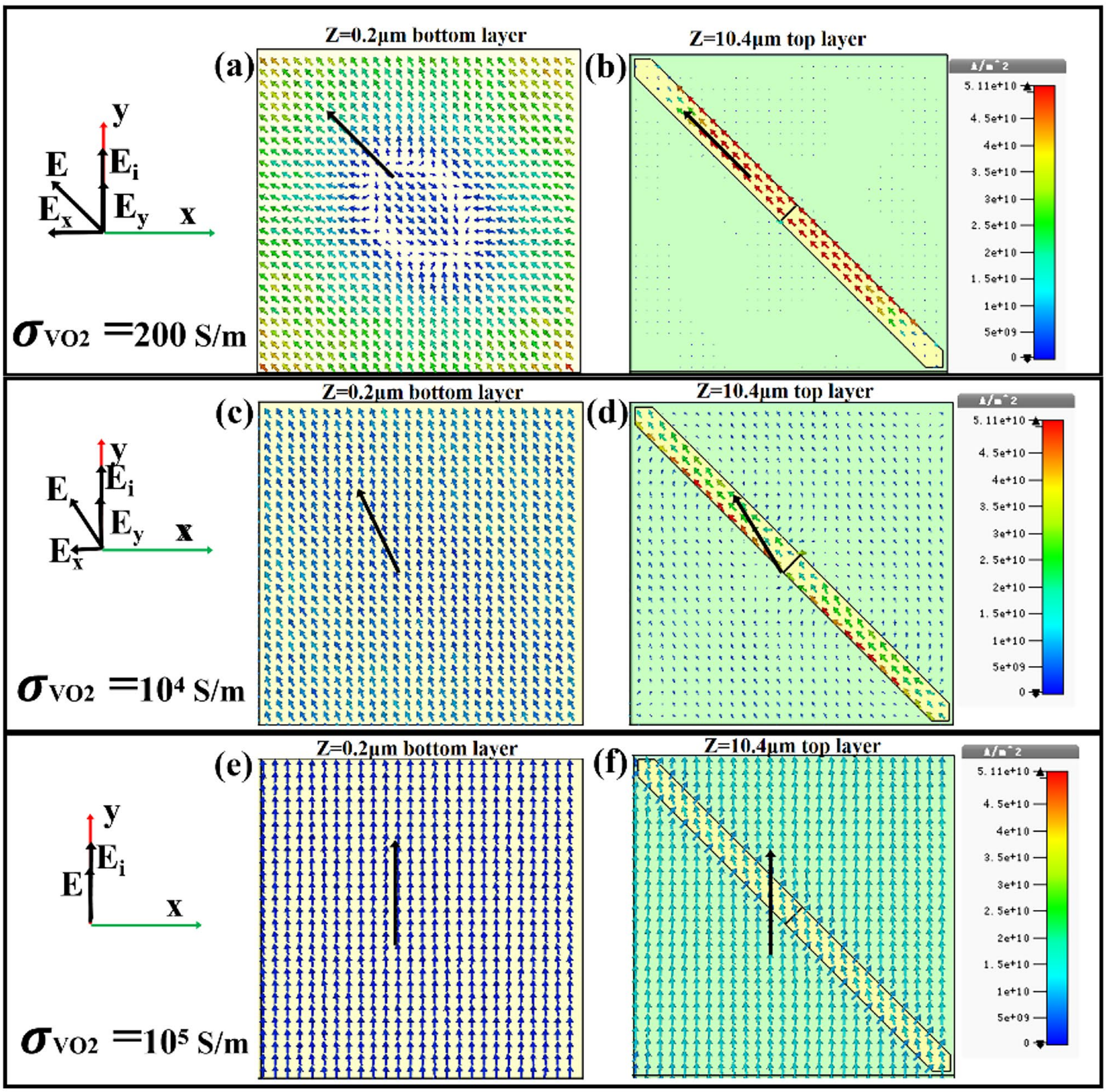

Fig. 5 Simulated current densities at 5.27 THz at the conductivities of 200, 10^4, and 10^5 S/m

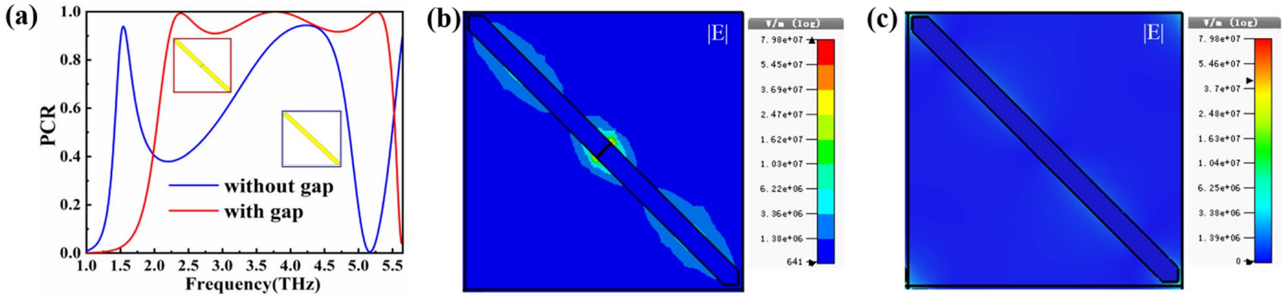

Fig. 6 (**a**) *PCR* with and without gap under incident *y*-polarized wave when $\sigma_{VO2}=200$ S/m. (**b**) and (**c**) Corresponding E-field map with and without gap $\sigma_{VO2}=200$ S/m at 5.27 THz

To understand the physic mechanism, the current densities of incident *y*-polarized wave are depicted as shown in Fig. 5. The conductivities of 200, 10^4, and 10^5 S/m at 5.27 THz are taken as example to describe thermal control effects. It is obviously that strong parallel currents called electric resonance [29–33] can be observed between the top and bottom layer in Fig. 5(a) and (b) at the conductivity of 200 S/m. The decomposed E_x component of induced E contributes to cross-polarization conversion. The E_y component of induced E has no impact on polarization for its same direction with incident E_i [34]. However, the current densities reflect gradually weakly between top and bottom layer when σ_{VO2} increases from 10^4 to 10^5 S/m as shown in Fig. 5(c), (d) and (e), (f). Moreover, induced E rotates parallel to incident E_i gradually from Fig. 5(c), (d) to (e), (f). Thus, it can be inferred that the incident wave can change from penetrating state to not penetrating the top layer state with utilizing the thermal controllable VO_2. In other words, as the temperature increases, the *y* to *x* cross-polarized component conversion decreases sharply.

Last but not least, in connection to discussion above, to further reflect the cleverly design characterized with a slit, relevant theory analysis on polarization converter metadevice with and without gap has been investigated in Fig. 6. Obviously, we can see that enhanced polarization conversion effect based on single-layer metadevice with gap occurs, while it disappear when the metadevice without gap. Of course, also, the micro-mechanism about corresponding E-field map [35] with and without gap has been discussed. Obviously, for the gap contained shown in Fig. 6(b), the E-field concentrates at the gap position of the inclined resonator, while E-field concertation at connection section without gap is nearly zero in Fig. 6(c), transporting certain amount of charges to two corners of the inclined resonator. This result is consistent with charge transfer for nanoscale system [36], further reflecting low conversion efficiency. All in all, the specific designed metadevice just yet achieve high polarization conversion efficiency with tunable bandwidth.

Conclusions

Based on metamaterial, a simply single-layer and tunable reflective polarization converter is proposed in THz spectrum, which composed of vanadium dioxide film (VO_2) inserted by a two-corner-cut square patch resonator with a slit and reflective ground layer. The calculated results show that high *PCR* (above 90%) can be obtained within the frequency range from 2.22 to 5.42 THz for the incident linear and circular polarization wave. In addition, the dynamic thermal changed polarization converter can also be accomplished by adjusting the conductivities of VO_2. To be demonstrated, the mechanism of tunable polarization conversion is also analyzed by investigating the current densities at the top and bottom layer under the condition of changeable conductivities. Last but not least, the reason for adding a slit on middle resonator has been illustrated in comprehensively. According to analysis above, the designed metamaterial with cleverly specific assemble could be applied in the area of temperature-controlled sensing, THz wireless communication, tunable polarized devices.

Author Contribution All the authors have participated in conceiving the idea, designing and simulating the structure, obtaining the results, and revising process. All the authors gave the final approval of the version to be submitted.

Funding This work is supported by Major Science and Technology Project of Anhui Province in China under grant 202003a05020031, Key Research and Development Plan of Anhui Province in China under grant 202004a05020023, School-level Scientific Research Project of Huainan Normal University under grant 2021XJYB027 and The second batch of Huainan City Guiding Science and Technology Plan Projects in 2021 (3624).

Data Availability All the data generated during and/or analyzed during the current study are available from the corresponding author on reasonable request.

Declarations

Ethics Approval All authors accepted.

Consent to Participate All authors accepted.

Consent for Publication All authors accepted.

Competing Interests The authors declare no competing interests.

References

1. Lee S, Baek S, Kim TT, Cho H, Lee S, Kang JH, Min B (2020) Metamaterials for enhanced optical responses and their application to active control of terahertz waves. Adv Mater 32:2000250
2. Zhang X, Xu Q, Xia L, Li Y, Gu J, Tian Z, Ouyang C, Han J, Zhang W (2020) Terahertz surface plasmonic waves: a review. Advanced Photonics 2:014001
3. Ahmadivand A, Gerislioglu B, Ahuja R, Mishra YK (2020) Toroidal metaphotonics and metadevices. Laser Photonics Rev 14:1900326
4. Ahmadivand A, Gerislioglu B, Ahuja R, Mishra YK (2019) Terahertz plasmonics: the rise of toroidal metadevices towards immunobiosensings. Mater Today 32:108–130
5. Mousavi SA, Plum E, Shi J, Zheludev NI (2015) Coherent control of optical polarization effects in metamaterials. Sci Rep 5:8977
6. Ma HF, Wang GZ, Kong GS, Cui TJ (2015) Independent controls of differently-polarized reflected waves by anisotropic metasurfaces. Sci Rep 5:9605
7. Tang J, Xiao Z, Xu K, Ma X, Liu D, Wang Z (2016) Cross polarization conversion based on a new chiral spiral slot structure in THz region. Opt Quant Electron 48:111
8. Xu G, Yu F, Guo K, Shen F, Zhou H, Sun Y, Zhang X, Yin Z, Guo Z (2017) Tri-band polarization convertor based on the multi-layer metamaterial. Appl Phys A 123:654
9. Li H, Xiao B, Li HX, Yang H (2015) Multiple-band reflective polarization converter based on deformed F-shaped metamaterial. Phys Scr 90:35806
10. Zhang J, Tian J, Xiao S, Li L (2020) Methodology for high purity broadband near-unity THz linear polarization converter and its switching characteristics. IEEE Access 8:46505–46517
11. Cheng H, Chen S,Yu P, Li J, Xie B, Li Z, Tian J (2013) Dynamically tunable broadband mid-infrared cross polarization converter based on graphene metamaterial. Appl Phys Lett 103:223102
12. Zhang DQ, Shu FZ, Jiao ZW, Wu HW (2021) Tunable wave plates based on phase-change metasurfaces. Opt Express 29:7494
13. Zhang K, Liu Y, Lin S, Xia F, Kong W (2020) Actively tunable bi-functional metamirror in THz band. Opt Lett 46:464–467
14. Sofi MA, Saurav K, Koul SK (2021) A linear to circular polarization reconfigurable converter based on frequency selective surface. Microw Opt Technol Lett 63:1425–1433
15. Yan D, Meng M, Li J, Li J, Li X (2020) Vanadium dioxide-assisted broadband absorption and linear-to-circular polarization conversion based on a single metasurface design for the THz wave. Opt Express 28:29843–29854
16. Wang D, Zhang L, Gu Y, Mehmood MQ, Gong Y, Srivastava A, Jian L, Venkatesan T, Qiu CW, Hong M (2015) Switchable ultrathin quarter-wave plate in THz using active phase-change metasurface. Sci Rep 5:15020
17. Liu M, Hwang HY, Tao H, Strikwerda AC, Fan K, Keiser GR, Sternbach AJ, West KG, kittiwatanakul S, Lu J, Wolf SA, Omenetto FG, Zhang X, Nelson KA, Averitt RD (2012) THz-field-induced insulator-to-metal transition in vanadium dioxide metamaterial. Nature 487:345–348
18. Zhao JX, Song JL, Zhou Y, Liu YC, Zhou JH (2020) Switching between the functions of half-wave plate and quarter-wave plate simply by using a vanadium dioxide film in a THz metamaterial. Chin Phys Lett 37:35–39
19. Song Z, Zhang J (2020) Achieving broadband absorption and polarization conversion in the same frequency band. Opt Express 28:2487–12497
20. Li J, Zheng C, Li J, Zhao H, Hao X, Xu H, Yue Z, Zhang Y, Yao J (2021) Polarization-dependent and tunable absorption of THz wave based on anisotropic metasurface. Opt Express 29:3284–3295
21. Liu M, Plum E, Li H, Li S, Xu Q, Zhang X, Zhang C, Zou C, Jin B, Han J, Zhang W (2021) Temperature-controlled optical activity and negative refractive index. Adv Funct Mater 31:2010249
22. Ren Y, Zhou T, Jiang C, Tang B (2021) Thermally switching between perfect absorber and asymmetric transmission in vanadium dioxide-assisted metamaterials. Opt Express 29:7666–7679
23. Zhang J, Wang G, Zhang B, He T, He Y, Shen J (2016) Photoexcited broadband tunable THz metamaterial absorber. Optical Materials Optical Materials 54:32–36
24. Xiao Z, Zou H, Zheng X, Ling X, Wang L (2017) A tunable reflective polarization converter based on hybrid metamaterial. Opt Quant Electron 49:401–401
25. Lv TT, Li YX, Ma HF, Zhu Z, Li ZP, Guan CY, Shi JH, Zhang H, Cui TJ (2016) Hybrid metamaterial switching for manipulating chirality based on VO2 phase transition. Sci Rep 6:23186
26. Jepsen PU, Fischer BM, Thoman A, Helm H, Suh JY, Lopez R, Haglund Jr RF (2006) Metal-insulator phase transition in a VO2 thin film observed with terahertz spectroscopy. Phys Rev B 74:205103
27. Wen QY, Zhang HW, Yang QH, Xie YS, Chen K, Liu YL (2010) Terahertz metamaterials with VO2 cut-wires for thermal tunability. Appl Phys Lett 97:021111
28. Wen QY, Zhang HW, Yang QH, Chen Z, Long Y, Jing YL, Lin Y, Zhang PX (2012) A tunable hybrid metamaterial absorber based on vanadium oxide films. J. Phys. D: Appl Phys 45:235106
29. Wang BX (2017) Quad-band THz metamaterial absorber based on the combining of the dipole and quadrupole resonances of two SRRs. IEEE J Sel Top Quantum Electron 23:4700107
30. Hentschel M, Weiss T, Bagheri S, Giessen H (2013) Coupling of solid and inverse plasmonic structures. Nano Lett 13:4428–4433
31. Liu N, Guo H, Fu L, Kaiser S, Schweizer H, Giessen H (2008) Three-dimensional photonic metamaterials at optical frequencies. Nat Mater 7:31–37
32. Liu N, Giessen H (2010) Coupling effects in optical metamaterials. Angew Chem Int Ed Engl 49:9838–9852
33. Zhang Z, Wang J, Fu X, Jia Y, Chen H, Feng M, Zhu R, Qu S (2021) Single-layer metasurface for ultra-wideband polarization conversion: bandwidth extension via Fano resonance. Sci Rep 11:585
34. Zhao JC, Cheng YZ (2017) Ultra-broadband and high-efficiency reflective linear polarization convertor based on planar anisotropic metamaterial in microwave region. Optik 136:52–57
35. Ahmadivand A, Sinha R, Gerislioglu B, Karabiyik M, Pala N, Shur M (2016) Transition from capacitive coupling to direct charge transfer in asymmetric terahertz plasmonic assemblies. Opt Lett 41:5333–5336
36. Wen F, Zhang Y, Gottheim S, King NS, Zhang Y, Nordlander P, Halas NJ (2015) Charge transfer plasmons: optical frequency conductances and tunable infrared resonances. ACS Nano 9:6428–6435